Toward Economical Seawater-Based Methane Hydrate Formation at Ambient Temperature: A Combined Experimental and Computational Study

Ahmed Omran, Nikolay Nesterenko, Arnold A Paecklar, Nicolas Barrier, Valentin Valtchev

Toward Economic Seawater-based Methane Hydrate Formation at Ambient Temperature : A Combined Experimental and Computational Study

Ahmed Omran,[†] Nikolay Nesterenko,[‡] Arnold A. Paecklar,[¶] Nicolas Barrier,[¶] and Valentin Valtchev[*,§]

†*Normandie Université, ENSICAEN, UNICAEN, Laboratoire Catalyse et Spectrochimie (LCS), 14050, Caen, France*

‡*TotalEnergies One Tech Belgium, Zone Industrielle C, 7181, Seneffe, Belgium*

¶*Normandie Université, ENSICAEN, UNICAEN, CNRS, Laboratoire de Cristallographie et Science des Matériaux (CRISMAT), 14050 Caen, France*

§*Normandie Université, ENSICAEN, UNICAEN, CNRS, Laboratoire Catalyse et Spectrochimie (LCS), 14050, Caen, France*

E-mail: valentin.valtchev@ensicaen.fr

Phone: + 33 (0)2 31 45 27 33

Abstract

Clathrate hydrates are emerging as a novel storage medium for safe and compact methane storage. However, their industrial-scale applicability is hindered by sluggish formation kinetics and intense energy cooling requirements. The present study is the first report on binary methane-tetrahydrofuran (THF) formation using the combination

of seawater and an unstirred reactor at ambient temperature (298.2 K) that would improve the process economics. Acidic zeolites with different Si/Al ratios (USY-40 and USY-10) as well as aliphatic (L-valine) and aromatic (L-tryptophane) amino acids are employed as environmentally benign kinetic hydrate promoters. The experimental study is combined with DFT calculations to shed light on the role of kinetic promoters in hydrate formation. The set of experimental data revealed that hydrophobic zeolites with a higher Si/Al ratio performed better than the more hydrophilic ones. Moreover, the aliphatic amino acid L-valine showed better kinetic promotion performance for hydrate formation in natural and artificial seawater than the aromatic amino acid L-tryptophan. The optimization of the experimental condition allowed a controlled hydrate growth boosting the gas uptake to 40 mmol gas/mol water, which is the highest reported under mild conditions using seawater. In addition, the induction time is reduced to less than 10 minutes, and a methane recovery of 97% is reached without any foaming signs. Thus, this study demonstrates the possibility of controlling the stochastic nature of nucleation and hydrate growth by properly manipulating the reaction system. Our results provide a better understanding of hydrate nucleation enhancement under realistic conditions and open the door for a possible application of these environmentally benign kinetic hydrate promoters (KHPs) for synthetic natural gas (SGH) on a continuous process and industrial scale.

Introduction

Global energy demand rapid increase and movement toward less carbon emission has emphasized the role of natural gas as a transitional and clean fossil fuel toward decarbonization [1–4]. Recent disturbances in the natural supply chain due to the pandemic and geopolitical developments highlighted the need for economic long-term methane storage [5,6]. Currently, the state-of-the-art technology of LNG (liquified natural gas) is limited by short-time storage due to the expensive cooling cost, and the need for large reserves as well as long-term con-

tracts[7–9]. To overcome the above challenges, 'zeolitic ice' or synthetic gas hydrate (SGH) that allows methane storage in a stable, recoverable, compact, and safe solid are considered[10,11]. Moreover, they enable the use of stranded and discrete gas resources such as flue and shale gases. However, the application of such promising material is hindered by slow kinetics and high formation condition economics[12,13]. Desalination costs combined with the energy-intensive hydrate formation cooling requirement and agitation impose a high capital overhead on SGH technology[14,15]. The above challenges could be faced by using accessible seawater instead of deionized water. However, the presence of salts such as sodium chloride and high temperature can impose a double inhibitory effect on hydrate synthesis[9].

Among different reactor configurations used to study methane hydrate formation, the stirring and unstirred reactor configurations were the most common ones. Stirred reactors were used to overcome mass transfer limitations and consequently enhance methane hydrate formation by continuously disturbing the gas-liquid interface where nucleation predominantly occurs[16]. In general, this results in a relatively shorter induction time. For example, Pahlavanzadeh *et al* investigated methane hydrate formation in the stirred reactor in presence of nanofluids at 275.15 K and 5 MPa. The induction time was about 15-50 mins while gas uptake did not exceed 0.06 mol gas/mol water[17]. However, most of the research studies in stirred reactors employed a bottom-mounted stirrer (usually a magnetic stirrer). Hydrate clusters tend to float up in such an arrangement, forming a thin layer that separates the gas from bulk water. This typical mass transfer causes a quick drop in gas uptake shortly after nucleation. Thus, for example, Linga *et al.* found that fixed bed silica sand performed better than the stirred reactor[18]. Recent studies such as Gootam *et al* showed that a top-mounted stirrer can improve the rate constant due to more efficient mixing[19]. However, scale-up studies that involved both heat and mass transfer analysis showed that the stirred-reactor configuration is not favorable for any significant economic scale-up[20]. This conclusion can be explained by the lower hydrate mass in water ($\leq$ 5 wt%), agitation energy cost as the slurry

thickens, and post-processing cost of filtration and packing[21]. On the other hand, unstirred and packed bed reactors showed better gas uptake and hydrate yield than the other reactor designs, including stirred reactor configuration[22,23].

Recently, a huge experimental effort has been directed to enhance methane hydrate kinetics from natural or simulated seawater (2.7-3.5 wt% NaCl) in non-stirred reactors[24,25]. To accelerate the hydrate formation rate in such inhibitory medium, kinetic promoters such as sodium dodecyl sulfate (SDS) and amino acids were used. For instance, Veluswamy *et al.* investigated the kinetic performance of amino acids for sII mixed methane/THF hydrate formation from saline water (3 wt% NaCl) at 283.2 K. The study showed a low concentration of leucine (200 ppm) could improve the hydrate kinetics at 5 MPa[26]. Pandey *et al.* investigated the kinetics of binary CH_4-THF hydrate formation in the presence and absence of 3 wt% NaCl under similar thermodynamic conditions. They observed "cobweb-like" hydrate formation with no significant drop in storage capacity at 283.2 K and 5 MPa in presence of salt. However, the authors stressed the need for higher driving forces and identifying better promoters and reactors to enable the saline solutions to have reasonable gas uptakes comparable to non-saline ones[27].

Although the above efforts were useful to understand hydrates of saline solutions, they are still far from economic feasibility due to the low formation temperature. At higher temperatures, SDS (sodium dodecyl sulfate) is commonly used to improve the extremely slow kinetics. In that case, the presence of SDS may be also accompanied by higher pressure (driving force) or associated with other kinetic promoters, or both. For example, Nesterov and Reshetnikov examined pure methane hydrate formation from saline water (3 wt%) in presence of 0.1 wt% SDS at 275 K. They found that SDS micelles did not form even if the pressure increased from 8 to 16 MPa[28]. Moreover, Inkong *et al.* tested co-promoters of SDS and amino acids for binary CH_4-THF sII hydrates from a saline solution of 3.5 wt% NaCl

at 8 MPa and 288 K. Despite the reduced induction time and increased hydrate formation rate in presence of SDS, it resulted in 50% reduction of methane uptake and hydrate yield compared to stand-alone amino acids[25,29]. Thus, the effect of SDS addition to saline water is the same in both sI and sII hydrate studies. In addition to the above adverse effects of SDS as kinetic hydrate promoter (KHP), it has been found that it is not practical for any practical scale-up application due to severe foam formation even at low concentrations[30]. Thus, there is a need to explore other KHPs that can avoid those drawbacks.

Some experimental studies have also investigated hydrate formation from seawater to approach more realistic conditions. For example, Kumar *et al.* examined sII hydrate formation from both seawater and simulated seawater (3 wt% NaCl) at 7.2 MPa and 283.2 K. They highlighted that real seawater ($\sim$ 2.7 wt% salinity) showed slightly less volumetric storage of 86.3 V/V than that saline water (3 wt% NaCl) of 89.2 V/V in presence of THF. They have also highlighted that sI hydrate from saline water (without THF) could not exceed 15.5 V/V even if the condition changed to 10 MPa and 274.2 K[31]. Veluswamy *et al.* emphasized the slight lower uptake in the case of natural seawater than an artificial one[26]. In another study, the same group investigated the effect of leucine and tryptophan for sII hydrate formation from both natural and artificial seawater and found that leucine resulted in higher gas uptake than tryptophan while natural seawater (2.72 wt% salinity) outperformed artificial one (3.0 wt%) in terms of total methane uptake and reaction rate[32].

In addition to amino acids, porous material that can act as nucleation sites that accelerate the nucleation process was employed as KHPs[33–41]. Among porous materials, zeolites are green materials with low cost, large surface area, tunable acidity and hydrophobicity, and above all high stability in aqueous medium[42,43]. The above properties of zeolites can significantly affect the kinetics of hydrate formation[44,45]. For example, the zeolite hydrophobicity and acidity can be tuned by changing Si/Al ratio , synthesis conditions or healing

the defect sites[46,47]. Moreover, zeolites are stable in aqueous medium compared to the most common MOFs which suffer from structural deformation with their metal-coordinated linkers replaced by water molecules[48]. In spite of the advantages mentioned above, only a few studies investigated their performance as KHPs with zeolite Na-X (FAU-type) were reported as the best performing zeolite compared to different ion-exchange forms (3A and 5A) of zeolite A (LTA-type). In all above cases SDS was added to the porous material to get satisfactory condition especially when the temperature increased close to ambient[49–52]. Recently, Omran *et al.* revealed that acidic zeolite (H-Y, FAU-type) exhibited superior KHP performance over the basic one 13X (Na-X, FAU-type) for at relatively mild pressure (6 MP) without the need for SDS[45]. While there are many studies that investigated saline-based hydrate formation at elevated pressures and lower temperatures[22], it has been rarely studied at ambient temperature. Bhattacharjee *et al.* studied the formation of methane-THF hydrates at ambient temperature (298.2 K) and moderate pressure (9.5 MPa) in presence of amino acids (L-arginine and L-tryptophan). However, they had to use 0.3 mol% TBAF (tetra-n-butylammonium fluoride) as a second thermodynamic promoter (THP) to obtain a maximum gas uptake of 29.30 mmol methane/mol of water as the reaction could survive more than 3-4 hours in those challenging conditions. In addition to the above chemicals, below-mounted agitation with a magnetic stirrer, at least at the beginning of hydrate nucleation, was necessary[53]. This combination of multiple chemical additives and agitation increased the overall cost of the process and may cancel out the expense saved from avoiding the desalination process.

The primary objective of this study is to enhance the economic feasibility of green methane hydrate formation by maximizing the gas uptake at conditions as close as possible under realistic conditions. To achieve that objective, we investigated (1) natural seawater-based mixed methane-THF hydrate formation in (2) non-stirred reactor configuration (packed-bed) at (3) ambient temperature (298.2 K), and (4) moderate pressure (9.5

MPa). To overcome these extreme inhibitory conditions, we employed single environmentally benign KHPs of amino acids, and acidic zeolites (USY-10 and USY-40). Furthermore, the promoting mechanism of those materials was studied with both DFT (density functional theory) calculations and detailed kinetic data.

Experimental Section

Material and apparatus

Methane (99.99% purity) was purchased from Linde Co., Tetrahydrofuran (THF, AR grade 99.99%) from Alfa Aesar, ultra-stable acidic zeolites (H-USY40 and H-USY10) with different Si/Al ratios were obtained from Zeolyst. Amino acids L-tryptophan (reagent grade, 99 %) and L-valine (reagent grade, 99%) were purchased from Alfa Aesar. Sodium chloride (reagent grade, 99%) was purchased from Sigma-Aldrich. Fresh desalinated water were prepared in LCS (Laboratoire Catalyse et Spectrochimie), France. Natural seawater (SW) was obtained from Ouistreham coast, Caen, France. Simulated seawater (SSW) was prepared with 3 %wt NaCl. The acidic form of zeolites was calcined at 450°C for 4 hours. THF 5.56 mol% solution or its mix with zeolite or amino acid were prepared in a volumetric flask.

The instrument used for methane hydrate formation and dissociation is shown in **Figure S1**. The set-up is composed of a 450 cm^3 high-pressure stainless-steel reactor (CR; Parr) immersed in a cooling bath. The reactor is immersed in a cooling bath whose temperature is controlled by an external refrigerator (ER; Julabo, F250) which circulates a glycol solution. The pressure and temperature measurement were monitored by a pressure transmitter (PT; UNIK 5000, GE) with a range of 0-30 MPa and 0.1 % global error and a K-type thermocouple (T) with ± 1.0 K accuracy, respectively. To monitor the data during different experiments, a data acquisition logger (DAQ; Nanodac, Eurotherm) was connected to a personal computer (PC) and collected the data every 10 seconds. To ensure reproducibility and consistency, each

experiment was repeated at least three times and average data is reported. All experiments were performed an isochoric quiescent system; i.e with a fixed total volume of gas and solution or hydrate in a closed system.

Characterization

The zeolite powders were characterized using powder X-ray diffraction (PXRD), scanning electron microscope (SEM), inductively coupled-atomic plasma emission spectroscopy (ICP-AES), and scanning electron microscopy (SEM) equipped with energy dispersive X-ray (EDX), and N_2-adsorption. The synthesized binary CH_4-THF hydrate was characterized by PXRD and C^{13} NMR. Composition analysis of natural seawater was obtained from ICP. Methods, procedures, calculations, and equipment are detailed in the supporting information.

Experimental Procedure and Calculations

All experiment has been performed at ischoric and isothermal conditions. Detailed description of hydrate formation and recovery procedures and associated calculations are detailed in supporting information. Density functional theory (DFT) calculations[54] using the projected augmented wave (PAW) method and the standard pseudopotentials supplied by Quantum Espresso (QE) software[3,55,56]. A full description of the hydrate-zeolites systems, as well as calculation details, are shown in supporting information.

Results and discussion

Zeolite Promoters and Hydrate Characterization

N_2-adsorption measurements, PXRD, and SEM images confirmed the crystal structures of USY-40 and USY-10 zeolites as shown in **Table S1**, **Figure S2**, and **Figure S3**, respectively.

ICP-AES and EDX revealed that Si/Al ratio of USY-40 is 42 compared to 13 in the case of USY-10. For hydrate characterization, we first confirmed sII formation using PXRD analysis. In addition, C^{13} NMR measurements on the seawater-based binary hydrate were performed. Spectroscopic data revealed methane occupancy in 5^{12} small cages of sII as a sharp peak at -4.3 ppm while the other two peaks (26.2 and 69.0 ppm) indicate the large cage occupancy of THF as shown in **Figure S4**. Details on the zeolite promoter and hydrate characterization results are provided in supporting information.

Effect of zeolite promoters on mixed CH_4-THF hydrate formation

The kinetic performance of different promoters employed for mixed methane-THF hydrate formation using seawater (SW) is summarized in **Table1**, while similar results for freshwater (FW) and simulated seawater (SSW) are detailed in **Table S2**. We have listed the investigated key parameters including reactor configuration, total gas uptake, induction time, t_{90} (time taken for 90% completion of methane uptake), and recovery. For each system the hydrate synthesis was investigated at a constant pressure of 9.5 MPa and ambient temperature of 298.2 K. Such a realistic condition will ensure more than 80% reduction in cooling costs as estimated by Veluswamy *et al.*[10]. The pressure of 9.5 MPa has been chosen after several trials to ensure optimum gas uptake without compromising the economic feasibility. Previous studies showed that the reaction with seawater under these conditions could not be sustained for more than 4 hours with a maximum uptake below 30 mmol gas /mol of water despite stirring and utilization of multiple thermodynamic promoters[53]. To overcome that and boost the gas uptake, a special alloy of lightweight corrosion resistance metallic packing has been utilized to enhance heat transfer. Metallic packing has been successfully employed in literature to improve the thermal conductivity during hydrate formation[57,58].

To study the kinetic performance of zeolite promoters, USY-40 and USY-10 have been initially tested at 300 ppm concentrations and 9.5 MPa pressure. **Figure 1** compares the

Table 1: Summary of experiments carried out with THF 5.56 mol% seawater (SW) in the absence and presence of different promoters. In all listed experiments, temperature and initial pressure were 298.2 K and 9.5 MPa.

System	Experiment No.	Reactor Type	**Gas uptake(mmol gas/mol H_2O)**	Induction Time (min)	t_{90}[a]	**Revovery (%)**[b]
SW+ 5.56 mol % THF	A1	NSTR	20.93(±3.5)	13.10(±5.5)	403.70	97.30
	A2	NSTR	20.80(±1.5)	14.20(±3.8)	213.00	96.50
	A3	NSTR	20.20(±2.8)	15.70(±7.7)	375.00	96.30
SW+ 5.56 mol % THF+0.03% L-Tryptophan	B1	NSTR	29.57(±1.2)	7.70(±4.7)	271.30	98.00
	B2	NSTR	24.39(±2.6)	8.00(±1.8)	282.30	97.30
	B3	NSTR	28.70(±1.8)	7.50(±3.8)	241.50	96.70
SW+ 5.56 mol % THF+0.03% L-Valine	C1	NSTR	37.98(±1.5)	8.20(±2.7)	410.80	97.50
	C2	NSTR	35.28(±2.7)	7.20(±3.3)	409.00	97.20
	C3	NSTR	34.91(±2.9)	5.30(±2.7)	426.50	97.40
SW+ 5.56 mol % THF+0.03% US-Y-40	D1	NSTR	40.04(±1.4)	6.90(±1.8)	410.20	96.10
	D2	NSTR	38.67(±2.3)	5.20(±2.2)	410.20	97.90
	D3	NSTR	41.20(±2.7)	4.70(±3.5)	376.80	97.09
SW+ 5.56 mol % THF+0.03%US-Y-10	E1	NSTR	24.14(±1.3)	10.80(±4.2)	244.50	96.37
	E2	NSTR	20.03(±3.3)	11.20(±5.8)	267.70	96.41
	E3	NSTR	19.38(±2.1)	11.70(±4.7)	319.30	96.79

[a] average results of t_{90} varied within ±37 min

[b] average results of hydrate %recovery varied within ±1.54 %.

average gas uptake due to hydrate formation from natural seawater for 5.56 % blank THF solution along with 5.56 % THF solutions with USY-40 and USY-10 zeolites. Gas uptake has been plotted for the hydrate growth phase. In other words, time zero in that figure is considered the nucleation time. As shown in the figure, pure THF solution could achieve 20 mmol of gas/mol of water, similar to those uptakes reported by Bhattacharjee *et al.*[53] without stirring or using of additional promoters such as TBAF (tetra-n-butylammonium fluoride). Then, we tested two acidic zeolites of a similar framework (FAU) type to examine the effect of different Si/Al ratios and hydrophobicity on the performance of zeolites as kinetic hydrate promoters. The selection of acidic zeolites is based on our earlier experimental studies and DFT calculations that showed that the presence of an extra framework cation such as sodium could limit zeolite's promoting effect by binding to water molecules and breaking the intermolecular hydrogen bonds preventing water arrangement for hydrate cage formation[44,45,59]. Such behavior resulted in disturbing the intrinsic water network of hydrate cages. As seen in **Figure 1**, USY-10 (Si/Al ratio ≈ 13) zeolite showed a slightly better promoting effect than pure THF solution. One can observe that the induction time has been reduced by about 25% from 15 min to 11 min. However, the improvement is not high enough to be

noticed especially when it comes to gas uptake which has been increased only by about 10% compared to the blank THF solution. A worth noting observation is that in both cases the uptake is relatively low and the hydrate formation was difficult to be initiated and sustained.

On the hand, USY-40 (Si/Al ratio $\approx$ 42) showed a significant increase in overall kinetic performance and enhanced the gas uptake of synthetic gas hydrates (SGH). The induction time has been reduced to less than 7 mins or more than 50% compared to the blank THF solution. When compared to USY-10, it initially showed lower uptake for the first hour. However, the hydrate formation kinetics were accelerated and the reaction could be sustained for more than 9 hours despite the presence of salt (NaCl) at high concentrations in seawater. In this particular scheme, the action of acidic zeolite as kinetic hydrate promoter comes from (1) its role as a nucleation site and (2) its ability to extract hard cations such as sodium from the aqueous solution which allows smooth hydrate growth, and (3) it does not result in foaming. The presence of these hard cations can work as hydrate inhibitors even at low concentrations[60]. Moreover, the superior performance of USY-40 over USY-10 can be attributed to its higher Si/Al ratio. The relatively lower Si/Al ratio in the case of USY-10 resulted in a more hydrophilic nature and electrostatic structure that can reduce the water activity coefficient[61] which ultimately limits the promoting effect of zeolite as KHP. To further explain, one can say that the adsorption involves specific interaction between the water molecule and the hydrophilic centers in zeolite, which can be either a silanol group or a cation associated with the tetrahedrally coordinated aluminum[62]. Nguyen and Nguyen demonstrated that the moderate hydrophobicity of additive results in organizing the surrounding water into a clathrate-like structure and thereby promotes hydrate formation[44]. Recently, Denning *et al.* demonstrated that the more hydrophobic SSZ-13 (Si/Al ratio = 20) promoted 2.6 times more water-to-hydrate conversion than the hydrophilic SAPO-34 (Si/Al ratio = 0.6)[34]. Thus, the absence of sodium cation and the higher Si/Al ratio of USY-40 resulted in enhanced hydrophobicity. Combined with the additional gas-to-water

contact area indicated by the higher S_{ext} compared to USY-10, such hydrophobicity nature improved better orientation of water molecules for hydrate formation.

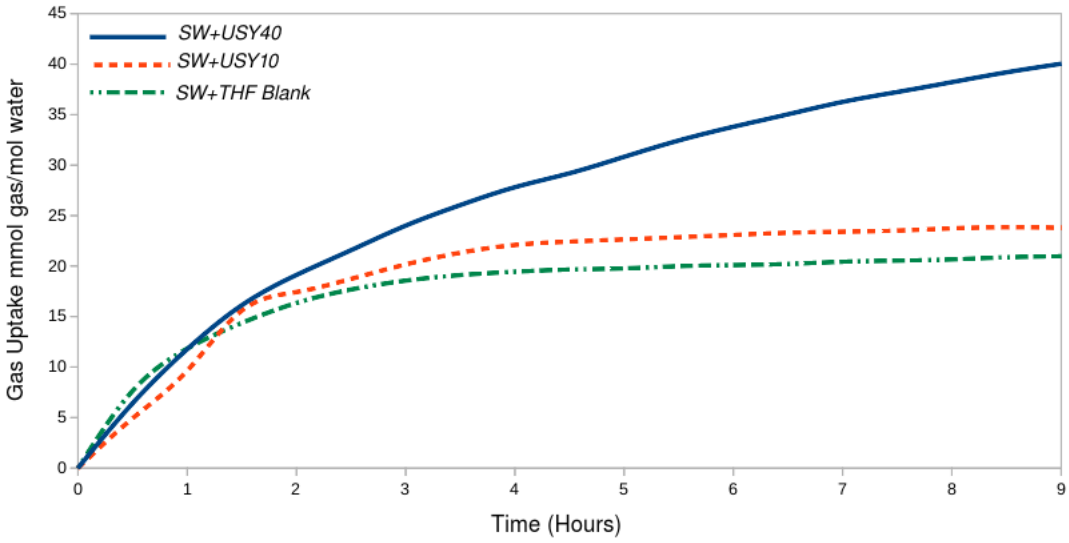

Figure 1: Comparison of average methane gas uptake owing to hydrate formation runs in the presence and absence of zeolite promoters: all solutions contain THF in the stoichiometric concentration of 5.56 mol% and hydrate synthesis temperature and pressure are 298.2 K and 9.5 MPa, respectively.

It is agreed that those salts such as NaCl have a thermodynamic inhibitory effect on hydrate formation in a way such as it is difficult to initiate the nucleation or maintain hydrate formation reaction[61,63]. Thus, the presence of these salts reduces the performance of zeolite hydrate promoters as illustrated in **Figure S6**. One can observe that zeolite kinetic promoter USY-40 performed better in natural seawater ($\approx$ 2.75 wt% salinity) compared to simulated seawater (SSW) which contains 3 wt% or 1.1 mol% NaCl. In spite of the initial higher methane uptake in the case of SSW, both natural and simulated seawater achieved the same methane uptake after about 4 hours. However, while the hydrate growth could not be sustained for more than 4 hours in the case of artificial seawater due to the high concentration of inhibitory NaCl salt, the methane uptake continued in the case of natural seawater. This can be explained by the presence of other salts in seawater that are potentially

less inhibitory to hydrate growth than NaCl. Moreover, the induction time increased in the case of simulated seawater compared to the natural one. The reduced t_{90} in the case of simulated seawater can be seen as a reflection of the reduced methane uptake compared to natural seawater. On the other hand, using pure water resulted in significantly enhanced hydrate growth kinetics and much higher methane uptake. This indicates the efficacy of USY-40 zeolite as KHP in absence of the inhibitory effect of salts.

Effect of Amino Acids Promoters on Mixed CH_4-THF Hydrate Formation

Amino acids are a class of eco-friendly compounds that has been recently investigated to accelerate the hydrate formation kinetics[64]. However, there is a contradiction in the literature about their role in the clathrate formation[65,66]. For example, Sa *et al.* showed that amino acids, especially the hydrophobic ones can work as effective kinetic inhibitors for methane hydrate[67], while studies such as Veluswamy *et al.* showed they could work as promoters if used at concentrations of 300 ppm[68]. Prasad and Kiran came also to the latest conclusion but for CO_2 clathrates[69]. Thus, in this study, we have investigated two non-polar hydrophobic amino acids as kinetic promoters at concentrations as low as 300 ppm: the aliphatic amino acid (L-valine) and aromatic amino acid (L-tryptophan). The selection of hydrophobic amino acids is based on previous studies that showed that they are likely to perform better than hydrophilic ones as KHPs[44,70,71]. Moreover, L-valine and L-tryptophan have been previously reported to enhance hydrate kinetics in saline environments in synergism with THF[29,32]. As shown in **Figure 2**, both the aliphatic (L-valine) and aromatic (L-tryptophan) showed kinetic promoting effect for mixed CH_4-THF hydrate formation at ambient temperature when compared to blank solution. The average induction time is slightly reduced in the case of L-valine compared to L-tryptophan. On the other hand, L-tryptophan showed initial higher methane uptake than L-valine. Such a high methane uptake sharply drops down after 4 hours while L-valine could sustain relatively higher methane uptake for about 9 hours. Thus, L-

valine could achieve higher final methane uptake of 36 mmol gas/mol water compared to 28 mmol gas/mol water in the case of L-tryptophan.

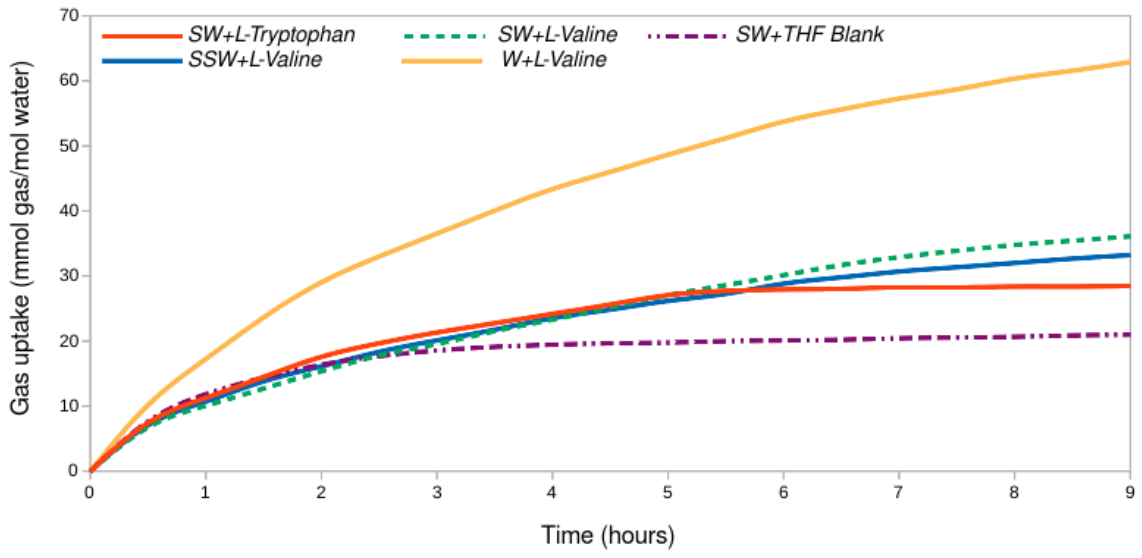

Figure 2: Comparison of average methane gas uptake owing to hydrate formation runs in the presence and absence of amino acid promoters: all solutions contain THF in the stoichiometric concentration of 5.56 mol% and hydrate synthesis temperature and pressure are 298.2 K and 9.5 MPa, respectively.

Finally, we have explored the behavior of L-valine in artificial seawater (3 wt% or 1.1 mol% NaCl) and freshwater. Similar to USY-40, L-valine showed slightly better performance in natural seawater than in artificial one as illustrated in **Figure 2**. Removing the effect of inhibitory salts, the gas uptake increased significantly by 75% to about 63 mmol gas/mol water. This reveals the real efficacy of L-valine as KHP. In addition, one can attribute the lower performance of amino acids in the seawater environment to the neutralizing effect of those salts, especially at ambient temperature. On the other hand, there was no foaming observed for both amino acids during hydrate dissociation. This crucial observation along with their kinetic performance, strengthened the possibility of their use to relieve surfactants

as KHPs due to their common structural similarities. To illustrate, while surfactant such as SDS is composed of a hydrophilic head and hydrophobic tail, L-valine is composed of hydrophilic carboxylic and amine groups associated with a hydrophobic side chain. In the next section, we will employ DFT calculations to further understand the relative kinetic performance of zeolite and amino for hydrate formation on the molecular level.

Molecular Level Interaction of Hydrate Cages with Promoter

We have utilized DFT calculations to shed light on the molecular level interactions leading to these results. *Ab initio* DFT has been commonly used in literature to report the effect of different promoters or inhibitors on hydrate formation[72,73]. In this study, DFT was employed to analyze zeolite-hydrate and amino acids-hydrate systems in terms of 5^{12} hydrate cage energies and geometrical changes upon their interaction either with finite zeolite clusters or with amino acid molecules. In addition, the energy of the host-guest cage system was calculated in the presence or absence of KHPs. The host-guest interactions are a key property that characterizes the clathrate stability[74] and can be assessed through interaction energy (ΔE^{HG}). This energy can be defined as follow:

$$\Delta E^{HG} = E(CH_4@5^{12}) - [E(CH_4) + E(5^{12})] \quad (1)$$

where $E(CH_4@5^{12})$, $E(CH_4)$, and $E(5^{12})$ are the energies of $CH_4@5^{12}$, methane molecule and the 5^{12} empty cage, respectively. The weak interactions such as H-bonding van der Waals forces dominate the hydrate, zeolite and amino acid systems interaction. Thus, the proper selection of exchange-correlation functional that capture those interactions is essential to represent those systems.

Thus, we initially calculated the interaction energy of methane with a small cage with three different levels of theory. The values were +2.03, -24.97 and -27.78 kJ/mol for revPBE,

rvv-10 and vdW-DF2 levels, respectively. While rvv-10 and vdW-DF2 exchange correlation functionals could successfully capture the dispersion forces, revPBE failed to accurately determine the host-guest interactions at all. Compared to -32.55 kJ/mol obtained by the highly accurate but computationally expensive MP2/6-311++G(d,p) level of theory[74], the interaction energy value obtained from vdW-DF2 shows better accuracy in describing the host-guest interaction compared to rvv-10. Consequently, we used it for all remaining calculations.

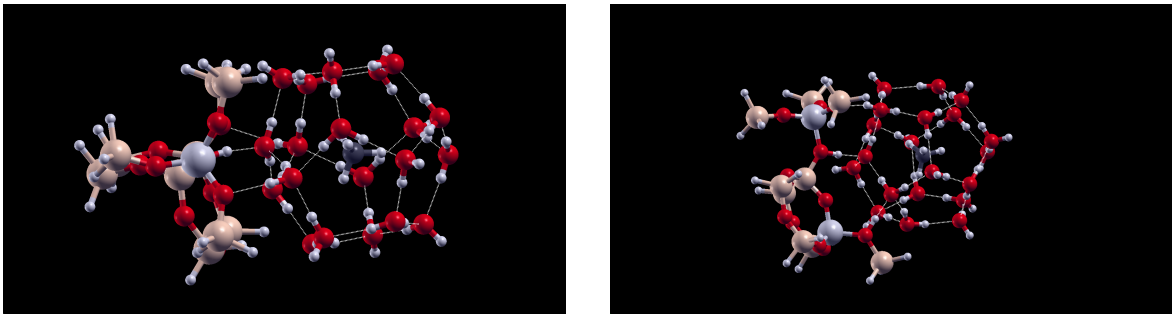

(a) USY-40 (high Si/Al cluster) (b) USY-10 (low Si/Al cluster)

Figure 3: Optimized configurations of small (5^{12}) cage with zeolite clusters of (a) USY-40 and (b) USY-10. Silicon, hydrogen, carbon, and aluminum atoms are shown in brown, white, black, and gray colors, respectively.

The optimized zeolite-cage structures are shown in **Figure 3**. We aimed to assess the degree of zeolite-clathrate interactions ($\Delta E^{Z\text{-}C}$) with different Si/Al ratios. The interaction energy is defined as follows:

$$\Delta E^{Z\text{-}C} = E(Z\text{-}CH_4@5^{12}) - [E(Z) + E(CH_4@5^{12})] \quad (2)$$

where $\Delta E^{Z\text{-}C}$ and E(Z) are the energy of the optimized Z-CH_4@5^{12} structure and isolated zeolite cluster, respectively. In this case, the lower energy values of the interaction between a host water molecule and the additive molecule indicate a more attractive interaction or inhibitory effect[75].

While the value for the low Si/Al cluster representing USY-10 zeolite is -189.957 kJ/mol, the high Si/Al cluster representing USY-40 showed only -149.69 kJ/mol. The relatively higher value in the case of a low Si/Al cluster indicates that the zeolite binding to the clathrate cage is much stronger and thus disturbs the hydrate growth. This slight stronger interaction could be explained as follows: with the presence of more Al atoms in the zeolite framework, the surface Brønsted acid sites (BAS) can form hydrogen bonds with hydrate cages as shown in **Figure 3**. Such an explanation is also applicable to hydrophilic surface silanol groups and agrees with the literature[76]. However, our previous studies showed that such hydrogen-bonding interactions due to BAS are much lower than that of alkali metal extra framework cations such as sodium which can cause the clathrate structure to collapse[45]. In particular, these cations possess high charge density and lower polarizability. Thus, they interact strongly with hydration shell around them with water dipoles pointing out from it[77]. Moreover, the higher hydrophilicity which can also disturb clathrate cage formation is another consequence of the lower Si/Al ratio. Accordingly, one can say that the USY-10 zeolite strongly binds to the clathrate cage and disturbs the hydrate growth due to its high Al content and thus higher hydrophilicity which agrees with the experimental observations. On the other hand, the effect of USY-40 zeolite particles as nucleation sites that enhance heterogeneous nucleation prevailed as the more hydrophobic acidic zeolite helped the water surrounding molecules to arrange for hydrate formation and promoted further cage growth.

Similarly, as illustrated in **Figure S7**, we have studied the interaction of both L-valine and L-tryptophane molecules with hydrate cage. The promoting effect of amphipathic amino acids depends on their chemical structure and relative hydrophobicity[44]. Our results showed that the aliphatic amino acid (L-valine) has interaction energy of -31.51 kJ/mol compared to -49.49 kJ/mol for aromatic amino acid (L-tryptophan). The more negative interaction energy in the case of L-tryptophan agrees well with our experimental observation that showed less methane uptake in the case of L-tryptophan despite the higher initial kinetic performance.

The optimized structures showed that while hydrate cage disturbance L-tryptophan could be attributed to hydrogen bonding with both the amino group and secondary amine group, it comes only from the amino group in the case of L-valine. In addition, one can attribute these promoting effects of L-valine to its relatively higher hydrophobicity. According to Kyte and Doolittle, the hydrophobicity value of L-valine (+4.2) compared to (-0.9) in the case of L-tryptophan[78]. Thus, based on computational data and experimental observations, one can conclude that the hydrophobic aliphatic group in L-valine enhanced the local water structure and create an increased gas concentration around the amino acid which is finally reflected in higher gas uptake and more sustained kinetics.

Controlling Hydrate Growth Phase: A Step Toward Flow Chemistry of Hydrate Process

One of the main objectives of this study is to give engineering and technological perspectives on economic methane hydrate formation on an industrial scale. To achieve that goal, we have chosen realistic conditions (seawater and ambient temperature) and made technological choices (non-stirred tank reactor, selection of low cost green promoters, and pressure below 10 MPa) to boost the process economics as detailed in the introduction. However, while our approach could reduce the induction time, enabled sustained hydrate growth, and increased the gas uptake in extremely inhibitory conditions compared to literature as illustrated at **Figure 4** , we are aware that the reaction time is still too long for a typical economic bath process.

Traditionally, the laboratory scale studies of hydrate formation are performed to increase the gas uptake in the shortest time possible. However, when it comes to pilot and industrial scales, establishing a continuous process or "flow chemistry" could save costs by eliminating multiple start-ups and shut-downs between different batches and low maintenance costs, among other reasons discussed in the literature[79]. However, continuous process requires a

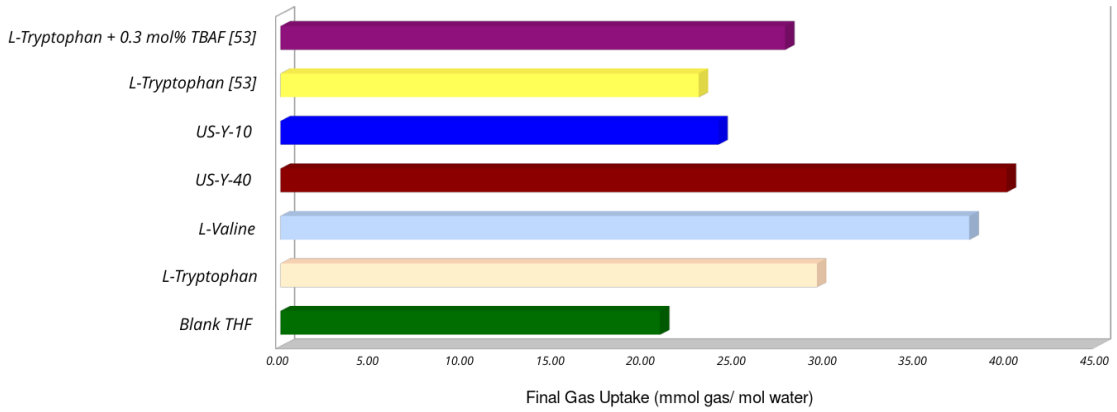

Figure 4: Comparison of average methane gas uptake owing to seawater-basted hydrate formation in this work compared to literature[53]: all solutions contain THF in stoichiometric concentration of 5.56 mol% and hydrate synthesis temperature and pressure are 298.2 K and 9.5 MPa, respectively.

steady-state process with controlled reaction conditions. In this study, we could achieve a controlled hydrate growth phase during the batch reaction by carefully selecting the proper reaction systems (reactants, reactor, and P-T condition) as shown in **Figure S8**. This temperature control within a tight range could eliminate the usual sudden, uncontrolled and stochastic hydrate growth associated with hydrate nucleation. With such controlled behavior, it is possible to extend the process from batch to continuous hydrate production.

Finally, there is naturally inherited lower gas uptake in seawater than in freshwater due to the inhibitory effect of salts regardless of the change in the reaction system. While higher gas uptake is an advantage for stationary storage, it bears challenges in hydrate transportation either within the hydrate production facility or outside. Previous experimental and computational observations showed a greater tendency for brittleness as the hydrate saturation increased[80,81]. Thus, increasing the gas uptake in seawater-based hydrate "slurry" while maintaining reasonable brittleness gives them an advantage during transporting hydrates without plugging the pipelines within the hydrate production plant or outside for long distances. Moreover, the above study addess the economic challenges associated with

the process. At similar hydrate formation conditions (300 K and 6 MPa), Javanmardi *et al.* earlier economic simulation studies of showed that pure water SGH process can reduce the capital cost for natural gas transportation by 48% compared to LNG especially with stranded gas resource[82]. Thus, the above study is an important step toward the feasible process. Furthermore, detailed and updated economic analysis are ongoing to accurately evaluate the process using seawater.

Conclusions

The goal presented study is to provide a molecular and macroscopic understanding of the role of green promoters of acidic zeolites and amino acids as kinetic hydrate promoters. To boost the reaction economics, we investigated binary methane-THF formation using both natural and simulated seawater in the unstirred reactor at ambient temperature (298.2 K) for the first time. Two types of environmentally benign kinetic hydrate promoters, acidic zeolites with different Si/Al ratios (USY-40 and USY-10) and amino acids (L-valine and L-tryptophane), were employed. Despite the challenging, extremely inhibitory environment due to the presence of salts and high temperature, the presence of green kinetic hydrate promoter was able to enhance hydrate formation kinetics and methane uptake. Our experimental results showed that zeolite (USY-40) with high Si/Al showed superior gas uptake than the low Si/Al zeolite (USY-10). DFT calculation showed that (USY-10) disturbed the hydrate cage due to its higher hydrophilicity and hydrogen bonding with surface BAS. On the other hand, the hydrophobic zeolite (USY-40) promoted the hydrate formation as it works to arrange water surrounding molecules for hydrate formation. The aliphatic amino acid L-valine showed better kinetic promotion performance and higher gas uptake in hydrate formation than the aromatic amino acid of L-tryptophan. The computational investigation revealed that the relatively less hydrophobic and aromatic L-tryptophan slightly disturbed the hydrate growth due to hydrogen bonding between the amino and secondary amine groups

and the local cage structure. On the other hand, the more hydrophobic aliphatic L-valine strengthened the local organization of the cage water structure. The use of aminoacids resulted in a substantial reduction of induction times to less than 10 minutes, and a methane recovery of 97%. The later being the highest gas uptake (40 mmol gas/mol water) reported under those challenging conditions. Finally, we have shown that the nucleation process can be controlled to a steady-state by selecting the proper reaction system, which paves the way for continuous hydrate production on an industrial scale. Our results provide a better understanding of hydrate nucleation enhancement under realistic conditions and open the door for a possible application of these green KHPs for SGH on the industrial scale.

Acknowledgement

The authors thank CRIANN (Centre Régional Informatique et d'Applications Numériques de Normandie) Normandy, France for providing the computing resources and the Industrial Chair ANR-TOTAL "NanoClean Energy" (ANR- 17-CHIN-0005-01) for the financial support. The authors also are grateful for Valérie RUAUX for her help with seawater analysis.

Supporting Information Available

Table summarizing the experiments carried out with THF 5.56 mol% water (FW) and simulated seawater (SSW), table of textural measurement for zeolite promoters obtained from Nitrogen adsorption measurements, table of ICP-AES for the zeolite promoters, table of EDX measurements of zeolite promoters, table of French Normandy region seawater composition analysis. Schematic diagram of hydrate formation and dissociation setup, figure of PXRD pattern of USY-10 and USY-40, Figure of ^{13}C MAS NMR spectra of seawater-based binary CH_4+THF hydrate (structure II) synthesized at 298.2 K , SEM images of (a) USY-10 and (b) USY-40, figure of PXRD pattern of mixed CH_4-THF clathrate, figure of Comparison of average methane gas uptake owing to hydrate formation runs in presence USY-40 zeolite

using seawater, simulated seawater and pure water, figure of Optimized configurations of small (5^{12}) cage with zeolite clusters of (a) L-tryptophan and (b) L-valine, and figure of P-T profile of (a) typical CH_4-THF hydrate formation from fresh water at 7 MPa and 283.2 K and (b) seawater-based hydrate formation using USY-valine as KHP at this work.

The following files are available free of charge.

- Filename: Supporting information

References

(1) Hafezi, R.; Akhavan, A. N.; Pakseresht, S.; A. Wood, D. Global natural gas demand to 2025: A learning scenario development model. *Energy* **2021**, *224*, 120167.

(2) Omran, A.; Yoon, S. H.; Khan, M.; Ghouri, M.; Chatla, A.; Elbashir, N. Mechanistic insights for dry reforming of methane on cu/ni bimetallic catalysts: DFT-assisted microkinetic analysis for coke resistance. *Catalysts* **2020**, *10*, 1–16.

(3) Omran, A. S. DFT Study of Copper-Nickel (111) Catalyst for Methane Dry Reforming. Ph.D. thesis, (Master Disseration)Texas A & M, 2019.

(4) Omran, A.; Ghouri, M.; Elbashir, N. DFT study of Copper-Nickel (111) Catalyst for Methane Dry Reforming. Third International Computational Science and Engineering Conference. Doha, Qatar, 2019.

(5) Kumar, A.; Singh, P.; Raizada, P.; Hussain, C. M. Impact of COVID-19 on greenhouse gases emissions: A critical review. *Sci. Total Environ.* **2022**, *806*, 150349.

(6) Sesini, M.; Giarola, S.; Hawkes, A. D. Solidarity measures: Assessment of strategic gas storage on EU regional risk groups natural gas supply resilience. *Appl. Energy* **2022**, *308*, 118356.

(7) Omran, A.; Nesterenko, N.; Valtchev, V. An Eco-Friendly Approach For Improved Methane Hydrate Kinetics In Near-Ambient Temperature and Moderate Pressure. ACS Research Conference : Chemistry and Chemical Engineering in MENA. Doha, Qatar, 2022.

(8) Javanmardi, J.; Nasrifar, K.; Najibi, S. H.; Moshfeghian, M. Natural gas transportation: NGH or LNG? *World Rev. Sci. Technol. Sustain. Dev.* **2007**, *4*, 258–267.

(9) Yin, Y.; Lam, J. S. L. Bottlenecks of LNG supply chain in energy transition: A case study of China using system dynamics simulation. *Energy* **2022**, *250*, 123803.

(10) Veluswamy, H. P.; Kumar, A.; Seo, Y.; Lee, J. D.; Linga, P. A review of solidified natural gas (SNG) technology for gas storage via clathrate hydrates. *Appl. Energy* **2018**, *216*, 262–285.

(11) Omran, A.; Nesterenko, N.; Valtchev, V. Ab initio Mechanistic Insight into the Stability, Diffusion, and Storage Capacity of H2, CH4, and CO2 in sI Clathrate Hydrate. European Congress and Exhibition on Advanced Materials and Processes - EUROMAT 2021. Virtual, Austria, 2021.

(12) Omran, A.; Nesterenko, N.; Valtchev, V. Zeolitic ice : A route toward net zero emissions. *Renew. Sustain. Energy Rev.* **2022**, *168*, 112768.

(13) Omran, A.; Nesterenko, N.; Valtchev, V. A Computational Insight of Guest Exchange Mechanism between CH4 and CO2 in SI Clathrate: CH4 Recovery and CO2 Storage Opportunities. TAMUQ-TotalEnergies Workshop "Successful Industry-Academia Collaboration in the Advancement of CO2 Utilization & Low Carbon Processes". Doha, Qatar, 2022.

(14) Pellegrini, L. A.; Moioli, S.; Brignoli, F.; Bellini, C. LNG technology: The weathering in above-ground storage tanks. *Ind. Eng. Chem. Res.* **2014**, *53*, 3931–3937.

(15) Shin, Y.; Lee, Y. P. Design of a boil-off natural gas reliquefaction control system for LNG carriers. *Appl. Energy* **2009**, *86*, 37–44.

(16) Ghaani, M. R.; Schicks, J. M.; English, N. J. A review of reactor designs for hydrogen storage in clathrate hydrates. *Appl. Sci.* **2021**, *11*, 1–16.

(17) Pahlavanzadeh, H.; Rezaei, S.; Khanlarkhani, M.; Manteghian, M.; Mohammadi, A. H. Kinetic study of methane hydrate formation in the presence of copper nanoparticles and CTAB. *J. Nat. Gas Sci. Eng.* **2016**, *34*, 803–810.

(18) Linga, P.; Daraboina, N.; Ripmeester, J. A.; Englezos, P. Enhanced rate of gas hydrate formation in a fixed bed column filled with sand compared to a stirred vessel. *Chem. Eng. Sci.* **2012**, *68*, 617–623.

(19) Gootam, D.; Gaikwad, N.; Kumar, R.; Kaisare, N. Modeling Growth Kinetics of Methane Hydrate in Stirred Tank Batch Reactors. *ACS Eng. Au* **2021**, *1*, 148–159.

(20) Mori, Y. H. On the scale-up of gas-hydrate-forming reactors: The case of gas-dispersion-type reactors. *Energies* **2015**, *8*, 1317–1335.

(21) Rossi, F.; Filipponi, M.; Castellani, B. Investigation on a novel reactor for gas hydrate production. *Appl. Energy* **2012**, *99*, 167–172.

(22) Linga, P.; Clarke, M. A. A Review of Reactor Designs and Materials Employed for Increasing the Rate of Gas Hydrate Formation. *Energy Fuels* **2017**, *31*, 30.

(23) Yin, Z.; Khurana, M.; Tan, H. K.; Linga, P. A review of gas hydrate growth kinetic models. 2018; `https://doi.org/10.1016/j.cej.2018.01.120`.

(24) Takeya, S.; Mimachi, H.; Murayama, T. Methane storage in water frameworks: Self-preservation of methane hydrate pellets formed from NaCl solutions. *Appl. Energy* **2018**, *230*, 86–93.

(25) Inkong, K.; Yodpetch, V.; Veluswamy, H. P.; Kulprathipanja, S.; Rangsunvigit, P.; Linga, P. Hydrate-Based Gas Storage Application Using Simulated Seawater in the Presence of a Co-Promoter: Morphology Investigation. *Energy and Fuels* **2022**, *36*, 1100–1113.

(26) Veluswamy, H. P.; Kumar, A.; Kumar, R.; Linga, P. Investigation of the kinetics of mixed methane hydrate formation kinetics in saline and seawater. *Appl. Energy* **2019**, *253*, 113515.

(27) Pandey, G.; Veluswamy, H. P.; Sangwai, J.; Linga, P. Morphology study of mixed methane-tetrahydrofuran hydrates with and without the presence of salt. *Energy and Fuels* **2019**, *33*, 4865–4876.

(28) Nesterov, A. N.; Reshetnikov, A. M. Combined effect of NaCl and sodium dodecyl sulfate on the mechanism and kinetics of methane hydrate formation in an unstirred system. *J. Nat. Gas Sci. Eng.* **2022**, *99*, 104424.

(29) Inkong, K.; Yodpetch, V.; Kulprathipanja, S.; Rangsunvigit, P.; Linga, P. Influences of different co-promoters on the mixed methane hydrate formation with salt water at moderate conditions. *Fuel* **2022**, *316*, 123215.

(30) Pang, W. X.; Chen, G. J.; Dandekar, A.; Sun, C. Y.; Zhang, C. L. Experimental study on the scale-up effect of gas storage in the form of hydrate in a quiescent reactor. *Chem. Eng. Sci.* **2007**, *62*, 2198–2208.

(31) Kumar, A.; Veluswamy, H. P.; Kumar, R.; Linga, P. Direct use of seawater for rapid methane storage via clathrate (sII) hydrates. *Appl. Energy* **2019**, *235*, 21–30.

(32) Veluswamy, H. P.; Linga, P. Natural Gas Hydrate Formation Using Saline/Seawater for Gas Storage Application. *Energy and Fuels* **2021**, *35*, 5988–6002.

(33) Borchardt, L.; Casco, M. E.; Silvestre-Albero, J. Methane Hydrate in Confined Spaces: An Alternative Storage System. *ChemPhysChem* **2018**, *19*, 1298–1314.

(34) Denning, S.; Majid, A. A.; Crawford, J. M.; Carreon, M. A.; Koh, C. A. Promoting Methane Hydrate Formation for Natural Gas Storage over Chabazite Zeolites. *ACS Appl. Energy Mater.* **2021**, *4*, 13420–13424.

(35) Khurana, M.; Yin, Z.; Linga, P. A review of clathrate hydrate nucleation. *ACS Sustain. Chem. Eng.* **2017**, *5*, 11176–11203.

(36) Said, S.; Govindaraj, V.; Herri, J. M.; Ouabbas, Y.; Khodja, M.; Belloum, M.; Sangwai, J. S.; Nagarajan, R. A study on the influence of nanofluids on gas hydrate formation kinetics and their potential: Application to the CO2 capture process. *J. Nat. Gas Sci. Eng.* **2016**, *32*, 95–108.

(37) Choi, J. W.; Chung, J. T.; Kang, Y. T. CO2 hydrate formation at atmospheric pressure using high efficiency absorbent and surfactants. *Energy* **2014**, *78*, 869–876.

(38) Pan, Z.; Liu, Z.; Zhang, Z.; Shang, L.; Ma, S. Effect of silica sand size and saturation on methane hydrate formation in the presence of SDS. *J. Nat. Gas Sci. Eng.* **2018**, *56*, 266–280.

(39) Wang, Y.; Lang, X.; Fan, S. Accelerated nucleation of tetrahydrofuran (THF) hydrate in presence of ZIF-61. *J. Nat. Gas Chem.* **2012**, *21*, 299–301.

(40) Rungrussamee, S.; Inkong, K.; Kulprathipanja, S.; Rangsunvigit, P. Comparative study of methane hydrate formation and dissociation with hollow silica and activated carbon. *Chem. Eng. Trans.* **2018**, *70*, 1519–1524.

(41) Zhang, G.; Liu, B.; Xu, L.; Zhang, R.; He, Y.; Wang, F. How porous surfaces influence the nucleation and growth of methane hydrates. *Fuel* **2021**, *291*, 120142.

(42) Peng, Y.; Krungleviciute, V.; Eryazici, I.; Hupp, J. T.; Farha, O. K.; Yildirim, T. Methane storage in metal-organic frameworks: Current records, surprise findings, and challenges. *J. Am. Chem. Soc.* **2013**, *135*, 11887–11894.

(43) Mahmoud, E.; Ali, L.; Sayah, A. E.; Alkhatib, S. A.; Abdulsalam, H.; Juma, M.; Al-Muhtaseb, A. H. Implementing metal-organic frameworks for natural gas storage. *Crystals* **2019**, *9*, 1–19.

(44) Nguyen, N. N.; Nguyen, A. V. Hydrophobic Effect on Gas Hydrate Formation in the Presence of Additives. *Energy and Fuels* **2017**, *31*, 10311–10323.

(45) Omran, A.; Nesterenko, N.; Valtchev, V. Revealing Zeolites Active Sites Role as Kinetic Hydrate Promoters: Combined Computational and Experimental Study. *ACS Sustain. Chem. Eng.* **2022**, *10*, 8002–8010.

(46) Palčić, A.; Valtchev, V. Analysis and control of acid sites in zeolites. *Appl. Catal. A Gen.* **2020**, *606*, 117795.

(47) Palčić, A.; Moldovan, S.; El Siblani, H.; Vicente, A.; Valtchev, V. Defect Sites in Zeolites: Origin and Healing. *Adv. Sci.* **2022**, *9*, 1–11.

(48) Burtch, N. C.; Jasuja, H.; Walton, K. S. Water stability and adsorption in metal-organic frameworks. *Chem. Rev.* **2014**, *114*, 10575–10612.

(49) Inkong, K.; Veluswamy, H. P.; Rangsunvigit, P.; Kulprathipanja, S.; Linga, P. Innovative Approach to Enhance the Methane Hydrate Formation at Near-Ambient Temperature and Moderate Pressure for Gas Storage Applications. *Ind. Eng. Chem. Res.* **2019**, *58*, 22178–22192.

(50) Zang, X. Y.; Fan, S. S.; Liang, D. Q.; Li, D. L.; Chen, G. J. Influence of 3A molecular sieve on tetrahydrofuran (THF) hydrate formation. *Sci. China, Ser. B Chem.* **2008**, *51*, 893–900.

(51) ZANG, X.; DU, J.; LIANG, D.; FAN, S.; TANG, C. Influence of A-type Zeolite on Methane Hydrate Formation. *Chinese J. Chem. Eng.* **2009**, *17*, 854–859.

(52) Kim, N.-J.; Park, S.-S.; Shin, S.-W.; Hyun, J.-H.; Chun, W. An experimental investigation into the effects of zeolites on the formation of methane hydrates. *International Journal of Energy Research* **2015**, *39*, 26–32.

(53) Bhattacharjee, G.; Veluswamy, H. P.; Kumar, R.; Linga, P. Seawater based mixed methane-THF hydrate formation at ambient temperature conditions. *Appl. Energy* **2020**, *271*, 115158.

(54) Kohn, W. Nobel lecture: Electronic structure of matter - Wave functions and density functional. *Rev. Mod. Phys.* **1999**, *71*, 1253–1266.

(55) Giannozzi, P. et al. QUANTUM ESPRESSO: A modular and open-source software project for quantum simulations of materials. *J. Phys. Condens. Matter* **2009**, *21*, 395502.

(56) Omran, A.; Nesterenko, N.; Valtchev, V. Ab initio mechanistic insights into the stability, diffusion and storage capacity of sI clathrate hydrate containing hydrogen. *Int. J. Hydrogen Energy* **2022**, *47*, 8419–8433.

(57) Kumar, A.; Sakpal, T.; Linga, P.; Kumar, R. Enhanced carbon dioxide hydrate formation kinetics in a fixed bed reactor filled with metallic packing. *Chem. Eng. Sci.* **2015**, *122*, 78–85.

(58) Kumar, A.; Kumar, R. Role of metallic packing and kinetic promoter in designing a hydrate-based gas separation process. *Energy and Fuels* **2015**, *29*, 4463–4471.

(59) Omran, A.; Nesterenko, N.; Valtchev, V. Revealing Acidic Zeolites: Role as New Kinetic Hydrate Promoters: A Combined Computational and Experimental Study. 37th meeting of French Group of Zeolite (GFZ). Vogüé, France, 2022.

(60) Kumar, A.; Sakpal, T.; Kumar, R. Influence of Low-Dosage Hydrate Inhibitors on Methane Clathrate Hydrate Formation and Dissociation Kinetics. *Energy Technol.* **2015**, *3*, 717–725.

(61) Sloan, E. D.; Koh, C. A. *Clathrate Hydrates Nat. Gases, Third Ed.*, 3rd ed.; CRC Press, 2007; pp 1–730.

(62) Chen, N. Y. Hydrophobic properties of zeolites. *J. Phys. Chem.* **1976**, *80*, 60–64.

(63) Makagon Yuri F., *Hydrates of Hydrocarbons*; Pennwell, 1997.

(64) Burla, S. K.; Pinnelli, S. R. P.; Sain, K. Explicating the amino acid effects for methane storage in hydrate form. *RSC Adv.* **2022**, *12*, 10178–10185.

(65) Roosta, H.; Dashti, A.; Hossein Mazloumi, S.; Varaminian, F. The dual effect of amino acids on the nucleation and growth rate of gas hydrate in ethane + water, methane + propane + water and methane + THF + water systems. *Fuel* **2017**, *212*, 151–161.

(66) Kim, K.; Cho, S. G.; Sa, J. H. Natural Hydrophilic Amino Acids as Environment-Friendly Gas Hydrate Inhibitors for Carbon Capture and Sequestration. *ACS Sustain. Chem. Eng.* **2021**, *9*, 17413–17419.

(67) Sa, J.-h.; Kwak, G.-h.; Lee, B. R.; Han, K.; Lee, K.-h. Hydrophobic amino acids as a new class of kinetic inhibitors for gas hydrate formation. *Sci. Rep.* **2013**, *3*, 1–7.

(68) Veluswamy, H. P.; Kumar, A.; Kumar, R.; Linga, P. Investigation of the kinetics of mixed methane hydrate formation kinetics in saline and seawater. *Appl. Energy* **2019**, *253*, 113515.

(69) Prasad, P. S.; Kiran, B. S. Are the amino acids thermodynamic inhibitors or kinetic promoters for carbon dioxide hydrates? *J. Nat. Gas Sci. Eng.* **2018**, *52*, 461–466.

(70) Bhattacharjee, G.; Linga, P. Amino Acids as Kinetic Promoters for Gas Hydrate Applications: A Mini Review. *Energy & Fuels* **2021**, *35*, 7553–7571.

(71) Wang, J.; Sun, J.; Wang, R.; Lv, K.; Wang, J.; Liao, B.; Shi, X.; Wang, Q.; Qu, Y.; Huang, H. Mechanisms of synergistic inhibition of hydrophilic amino acids with kinetic inhibitors on hydrate formation. *Fuel* **2022**, *321*, 124012.

(72) Lee, D.; Go, W.; Seo, Y. Experimental and computational investigation of methane hydrate inhibition in the presence of amino acids and ionic liquids. *Energy* **2019**, *182*, 632–640.

(73) Tariq, M.; Rooney, D.; Othman, E.; Aparicio, S.; Atilhan, M.; Khraisheh, M. Gas hydrate inhibition: A review of the role of ionic liquids. *Ind. Eng. Chem. Res.* **2014**, *53*, 17855–17868.

(74) Atilhan, M.; Pala, N.; Aparicio, S. A quantum chemistry study of natural gas hydrates. *J. Mol. Model.* **2014**, *20*, 1–15.

(75) Kumar, P.; Mishra, B. K.; Sathyamurthy, N. Density functional theoretic studies of host-guest interaction in gas hydrates. *Comput. Theor. Chem.* **2014**, *1029*, 26–32.

(76) Smirnov, K. S. A modeling study of methane hydrate decomposition in contact with the external surface of zeolites. *Phys. Chem. Chem. Phys.* **2017**, *19*, 23095–23105.

(77) Lukanov, B.; Firoozabadi, A. Specific ion effects on the self-assembly of ionic surfactants: A molecular thermodynamic theory of micellization with dispersion forces. *Langmuir* **2014**, *30*, 6373–6383.

(78) Kyte, J.; Doolittle, R. F. A simple method for displaying the hydropathic character of a protein. *J. Mol. Biol.* **1982**, *157*, 105–132.

(79) Holtze, C.; Boehling, R. Batch or flow chemistry? – a current industrial opinion on process selection. *Curr. Opin. Chem. Eng.* **2022**, *36*, 100798.

(80) Jendi, Z. M.; Servio, P.; Rey, A. D. Ideal Strength of Methane Hydrate and Ice Ih from First-Principles. *Cryst. Growth Des.* **2015**, *15*, 5301–5309.

(81) Yun, T. S.; Santamarina, C. J.; Ruppel, C. Mechanical properties of sand, silt, and clay containing tetrahydrofuran hydrate. *J. Geophys. Res. Solid Earth* **2007**, *112*, 1–13.

(82) Javanmardi, J.; Nasrifar, K.; Najibi, S. H.; Moshfeghian, M. Economic evaluation of natural gas hydrate as an alternative for natural gas transportation. *Appl. Therm. Eng.* **2005**, *25*, 1708–1723.

For Table of Contents Use Only

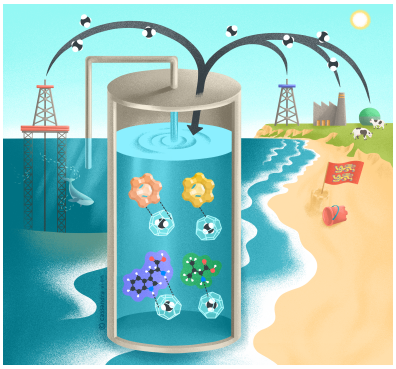

Synopsis

This study provides fundamental understanding for green kinetic promoters for accelerating sustainable methane storage in seawater-based clathrate hydrates.